DE GRUYTER OPEN DOI: 10.1515/aslh-2015-0001 Acta Silv. Lign. Hung., Vol. 11, Nr. 1 (2015) 9–25

The Effect of Soil Moisture on the Reflectance Spectra Correlations in Beech and Sessile Oak Foliage

Attila EREDICS[a*] – Zsolt István NÉMETH[b] – Rita RÁKOSA[b] – Ervin RASZTOVITS[a] – Norbert MÓRICZ[a] – Péter VIG[a]

[a] Institute of Environmental and Earth Sciences, Faculty of Forestry, University of West Hungary, Sopron, Hungary
[b] Institute for Chemistry, Faculty of Forestry, University of West Hungary, Sopron, Hungary

Abstract – Reflectance intensities of foliage are mostly due to biomaterials synthesised by plants. Adaptation to the continuously changing environment requires the regulated alteration of metabolic processes, which also influences the UV-VIS (Ultraviolet-Visible) and IR (Infra Red) spectra of leaves. For the calculation of various Vegetation Indices (VIs), e.g. NDVI (Normalized Difference Vegetation Index), the common practice is to use the reflectance spectrum of the whole foliage and when individual leaves of the same plant are sampled, an average VI is derived. On the contrary, our method exploits the small differences between individual leaves of the same plant, making use of the similar distributions of measured reflectance values. Using particular wavelength pairs, linear regressions of reflectance intensities have been investigated. The parameters of these regressions (slope and intercept) have been compared to the temporal variations of the environmental factors, such as temperature, vapour pressure deficit and soil moisture. By assessing the *sensitivity* of the regression coefficient (slope) to the changing environment, wavelength pairs can be selected whose *sensitivity* change reflects the effect of soil moisture deficit on the plant. Based on the state-dependent correlations of the reflectance spectra of plant foliage, a new concept is presented that is capable of indicating the level of environmental stress, e.g. drought stress.

drought stress / state-dependent correlation / UV-VIS and IR spectrometry

Kivonat – Talajnedvesség hatása bükk és kocsánytalan tölgy lombozat reflexiós spektrumainak korrelációira. A lombozat reflexiós intenzitásainak változását elsősorban a növény által előállított anyagok okozzák. A folyamatosan változó környezethez való alkalmazkodás megköveteli az anyagcsere-folyamatok szabályozott megváltoztatását, ami befolyásolja a levelek reflexiós spektrumát is az UV, látható és közeli infravörös tartományban. Különböző Vegetációs Indexek (VI) számításánál, mint pl. NDVI (Normalized Difference Vegetation Index), az általános gyakorlat szerint a teljes lombozat reflexiós spektrumát használják, vagy ha ugyanazon növény különböző leveleit mintázták, akkor egy átlagos VI-t származtatnak. Ezzel szemben módszerünk éppen a növény egyes levelei közötti kis különbségeket hasznosítja, kihasználva a mért reflexiós értékek hasonló eloszlását. Bizonyos hullámhosszpárokat kiválasztva, a mért reflexiós intenzitások lineáris regresszióit vizsgáltuk. A regressziós paramétereket (meredekség és tengelymetszet) összehasonlítottuk a környezeti hatások időbeli változásával, mint pl. hőmérséklet, légköri telítési hiány és talajnedvesség. A regressziós paraméter (meredekség) *érzékenységének* vizsgálatával olyan hullámhosszpárokat lehet

* Corresponding author: aeredics@yahoo.com; H-9400 SOPRON, Bajcsy-Zs. u. 4.

kiválasztani, melyek *érzékenység* változása tükrözi a talajnedvesség hiány növényre kifejtett hatását. Bemutatjuk az új módszer alkalmazhatóságát, amely a növényi lombozat reflexiós spektrumainak állapotfüggő korrelációján alapul, és amely képes a környezeti stressz, pl. szárazságstressz kimutatására.

szárazságstressz / állapotfüggő korreláció / UV-VIS és IR spektrometria

1 INTRODUCTION

Water is not only the media for metabolism, but also one of the key substrates in the cells. The effect of its deficit on various plant tissues and on the whole plant is one of the most studied phenomena in plant science. Recent publications about plant drought stress focused on the genetic background of drought resistance, the modifications of plant hormone systems and enzyme activities, the changing accumulation of biomaterials and the improvement of drought tolerance, among others. The test plants were usually various agricultural crops e.g. wheat, rice, soybeans, grapes and tomatoes. On the contrary, publications studying the effect of drought on trees, particularly by spectrometric methods, are less frequent (e.g. Filella – Peñuelas 1994, Peñuelas et al. 1997a,b, Pu et al. 2003).

The water status of trees can be measured by various methods, e.g. by leaf sampling and a pressure bomb (Scholander et al. 1965), stem psychrometer (Dixon – Tyree 1984) or the recently developed leaf patch clamp (Zimmermann et al. 2008). These methods are able to describe the instantaneous turgor pressure but reveal less about the long term effects of the drought stress, and may be very sensitive to the sampling time and conditions. On the other hand, the overall effect of the unfavourable conditions may be estimated by analysing the bio-production of the plant, e.g. yield, growth or accumulated dry material, but it demands a longer period or a full growing season in order to obtain significant differences.

The measurement of the leaf reflectance spectrum is a very promising way to characterize drought stress, and many different methods have been proposed to interpret the reflectance data. Many "high spectral resolution reflectance vegetation indices" have been developed to monitor biomass, phenology or physiology (Peñuelas – Filella 1998). These methods usually measure the reflectance at a few selected wavelengths and calculate a Vegetation Index (VI) from these reflectance values.

For example, a Simple Ratio (*SR*) can be used to estimate green biomass: $SR = R_{NIR} / R_{red}$, where *R* is reflectance and *NIR* stands for near infrared (Jordan 1969). A more robust and widespread method is the Normalized Difference Vegetation Index (*NDVI*) which is calculated as: $NDVI = (R_{NIR} - R_{red})/(R_{NIR} + R_{red})$ and used not only at ground level but also by airborne or satellite remote sensing (Rouse et al. 1973). *NDVI* is mainly sensitive to the green biomass (Gamon et al. 1995), but decent correlations are found with many other environmental or physiological variables. The exact wavelengths of *SR* and *NDVI* are somewhat arbitrary, and vary according to the spectral sensitivity of the sensor that is used or the goal of the investigation. Many practical uses of the *NDVI* have already been proposed and also used in industry, e.g. irrigation scheduling (e.g. Hunsaker et al. 2007, Aldakheel 2011), soil salinity management (e.g. Li et al. 2014), yield prediction (e.g. Teal et al. 2006, Moriondo et al. 2007) or fertilizer dosage adjustment (e.g. Stone et al. 1996, Crain et al. 2012).

Not only red and near infrared light, but many other wavelengths have been investigated, and various other VIs have been proposed for different purposes. *Table 1* summarises the most frequently used VIs along with the wavelengths they use. Many studies have been conducted to compare different VIs for specific application purposes, e.g. stress detection (e.g. Zarco-Tejada et al. 2004, Eitel et al. 2007, Pu 2008).

Table 1. The most frequently used Vegetation Indices along with their used wavelengths.

Vegetation Index (VI)	Abbrev.	Wavelengths	Reference
Simple Ratio	SR	NIR, red	Jordan (1969)
Normalized Difference Vegetation Index	NDVI	NIR, red	Rouse et al. (1973)
Normalized Difference Pigment Index	NDPI	430, 680	Baret et al. (1988)
Modified Chlorophyll Absorption in Reflectance Index	MCARI	550, 670, 700 or 550, 670, 800	Daughtry et al. (2000) or Haboudane et al. (2004)
Transformed CARI	TCARI	550, 670, 700	Haboudane et al. (2002)
Triangular Vegetation Index	TVI	550, 670, 750	Broge - Leblanc (2001)
Modified Triangular Vegetation Index	MTVI	550, 670, 800	Haboudane et al. (2004)
Renormalized Difference Vegetation I.	RDVI	670, 800	Roujean - Breon, (1995)
Soil Adjusted Vegetation Index	SAVI	670, 800	Huete (1988)
Improved SAVI with self-adjustment f.	MSAVI	670, 800	Qi et al. (1994)
Optimized Soil-Adjusted Vegetation I.	OSAVI	670, 800	Rondeaux et al. (1996)
Greenness Index	G	554, 677	-
Zarco-Tejada & Miller Index	ZMI	710, 750	Zarco-Tejada et al. (2001)
Simple Ratio Pigment Index	SRPI	430, 680	Peñuelas et al. (1995)
Normalized Phaeophytinization Index	NPQI	415, 435	Barnes et al. (1992)
3-band ratio	RATIO	975, 1200, 1750	Pu et al (2003)
Photochemical Reflectance Index	PRI	531, 570 or 528, 567	Gamon et al. (1992)
Normalized Pigment Chlorophyll Index	NPCI	430, 680	Peñuelas et al. (1994)
Carter ratios	Ctr	420, 695 or 605, 760 695, 760 or 710, 760	Carter (1994)
Lichtenthaler indices	Lic	450, 800 or 440, 690	Lichtenthaler (1996)
Structure-Independent Pigment Index	SIPI	445, 680, 800	Peñuelas et al. (1995)
Vogelmann indices	Vog	740, 720 or 715, 726, 734, 747 or 715, 720, 734, 747	Vogelmann et al. (1993)
Gitelson and Merzlyak	GM	550, 750 or 700, 750	Gitelson - Merzlyak (1997)
Water Index	WI	900, 970	Peñuelas et al. (1997b)
Normalized Difference Water Index	NDWI	860, 1240	Gao (1996)
Disease Water Stress Index	DSWI	547, 802, 682, 1657	Galvão et al (2005)

Not only indices can be calculated from individual reflectance values, but other properties of the spectra may also be analysed. The "Red Edge" method calculates the derivative of the reflectance spectra in the red - near infrared region, and seeks the wavelength of maximum slope. The Red Edge position and shape can be an indicator of the chlorophyll content of a plant and its water status, among others (e.g. Filella – Peñuelas 1994). Pu et al. (2003) assessed the water status of *Quercus agrifolia* leaves using different absorption characteristics, such as wavelength position, absorption depth and width, and also a 3-band ratio at 795, 1200 and 1750 nm.

A recent study by Tan et al. (2013) compared 54 different VIs to find the best predictor for the Fraction of Photosynthetically Active Radiation (FPAR) and found that not a single VI but a combination of two VIs showed the best results. The Index Database maintained by Henrich et al. (2012) currently (in 2015) registers 517 different indices used by remote sensing. Thirty three of them aim to assess the water content of vegetation and 10 are related to stress. Clearly, there is a lot of information buried in the reflectance spectra of leaves.

The method proposed by us offers a new approach to measure not only the short term, but also the cumulative effect of environmental stress with a potentially non-destructive method using the reflectance spectra of the leaves. It is based on the concept of the state-dependent correlation between biochemical variables by Németh et al. (2009a). If more leaves are sampled from the same plant for a VI measurement, the results of the individual leaves are not the same; therefore they are usually averaged to yield a single VI for the whole plant. On the contrary, our method exploits these small differences: the distribution of the measured reflectance values and the correlations between them.

2 THEORETICAL BACKGROUND AND RELATED WORK

Plants tend to adjust their physiological state to the actual conditions of their environment. The primary environmental factor is light intensity, which is different in the foliage from leaf to leaf; therefore the intensities of photosynthesis are different in the individual leaves. Thus, the concentrations of plant metabolites have a distribution pattern within the foliage. Environmental factors are able to modify the expected values and standard deviations of these metabolite distributions, and they can also distort the shape of these distributions. Thus, the effect of environmental conditions on foliage appears in the distribution functions of the metabolites. This means that the expected values and the standard deviations of the metabolites can change with alterations of environmental conditions; the distribution functions of the metabolites can move to and fro along their scales (Badáczy et al. 2011; Németh 2013).

If there are at least two metabolites in the metabolism whose amounts are regulated synchronously, then their types of distributions are necessarily the same, and the levels of metabolites correlate linearly to each other (Németh et al. 2009a). The theoretical equation of state-dependent correlation is deduced from the identity of the distributions of standardized metabolite levels, and this theoretical linear relationship can be approximated by regression analysis. The correlating metabolite concentrations provide a regression straight line. The slope and the intercept of this straight line are able to reflect alterations in the moments (expected value, standard deviation) of metabolite distributions induced by the environmental factors. Thus, the state-dependent regressions can indicate the modifications in environmental condition.

2.1 State-dependent regressions of the reflectance spectra

The reflectance spectrum, which is perceived as various colours in the visible range, pertains to the mixture of the different materials synthesized by leaf cells. Their amounts are the daily products of the photosynthesis that follow periodic alterations controlled by metabolic regulation. The diurnal variation of chlorophylls is one of the well-known cases of metabolic oscillations (e.g. Shimada 1958, Busheva et al. 1991). Similar diurnal changes have also been detected in other pigments, e.g. the xanthophylls (Adams – Demmig-Adams 1992).

Due to their significant light absorption in the visible and infrared regions, plant pigments, e.g. chlorophylls, carotenoids, xanthophylls, etc. are the main materials that dominate the reflection spectrum of the leaves. Since their distributions within the foliage are influenced by some environmental factors, the distributions of characteristic reflection (or absorption) intensities are also sensitive to environmental factors. Moreover, if the type of their distribution is the same, then the reflectance values belonging to various wavelengths will also linearly correlate and provide state-dependent regression straight lines. In conclusion, by measuring the spectra of leaves and deriving their state-dependent regressions, the alterations of the physiological states of the plants can be tracked.

If the synthesis and decomposition of two arbitrary metabolites in the plant cells are regulated synchronistically, the actual concentration values of such metabolites are not independent of each other. Moreover, if their synchronistic regulation has linear character, then their concentrations will also be related to each other in a linear manner. Absorbance values (A) obtained by spectroscopic measurement at particular wavelengths ($A_{\lambda 1}$ and $A_{\lambda 2}$) are proportional to the concentrations of these synchronously regulated metabolites and thus they are also linearly linked.

If the reflectance spectra have two such wavelengths (λ_1 and λ_2), whose absorbance intensities ($A_{\lambda 1}$ and $A_{\lambda 2}$) have the same type of distribution, then the standardised values of those absorbance intensities must be identical:

$$\frac{A_{\lambda 1}-\mu_1}{\sigma_1}=\frac{A_{\lambda 2}-\mu_2}{\sigma_2} \quad (1)$$

Where μ is the expected value and σ is the standard deviation of the A_λ absorbance intensity, measured at λ wavelength. Rearranging *Equation 1* produces the theoretical equation for the state-dependent correlation of reflectance spectra:

$$A_{\lambda 1}=\frac{\sigma_1}{\sigma_2}\cdot A_{\lambda 2}+\frac{\sigma_2\cdot\mu_1-\sigma_1\cdot\mu_2}{\sigma_2} \quad (2)$$

We investigated those wavelength pairs, whose absorbance intensities satisfy the equivalence criteria of *Equation 2*. This equation can be approximated by a linear regression: by fitting a straight line to the corresponding absorbance values:

$$A_{\lambda 1}=m\cdot A_{\lambda 2}+b \quad (3)$$

Where *m* is the slope and *b* is the intercept of the regression straight line.

2.2 Sensitivity and response time

On the base of the analogy between technological and biological control systems, the concept of *gain* can also be applied to physiological processes (Németh 2009b). Adaptation to different environmental conditions appears in altering the parameters *m* and *b*, which is visible from the different $A_{\lambda 1}$ to $A_{\lambda 2}$ linear regression. The *sensitivity* of the state-dependent regression can be evaluated by comparing the magnitude of the environmental changes e.g. temperature, to the changes of regression parameters *m* and *b*. If the relationship is more or less linear, then the slope of this straight line is hereafter called *"sensitivity"* (*S*). The control theory suggests that plants under stress exhibit greater *sensitivity* to disturbing environmental factors and thus *S* increases.

In a controlled environment such as a greenhouse, if we abruptly change (as a step function) only one influencing factor, e.g. temperature, we can measure the properties of the response: how intensely and how quickly the plant responds to reach a new quasi-stationer state. This measurement yields the *sensitivity* and the time constant of the system for the selected environmental parameter. However, under natural climatic conditions there are many influencing factors that change simultaneously and gradually. We can measure the response of the metabolic system, but the magnitude and duration of the influencing factor is not evident. To resolve this problem, the time series of the influencing environmental variables are needed with several samples at different times, which show the actual state of the metabolic system.

The response of the plant to the changing environment is relatively slow, so the physiological state of the plant does not closely follow e.g. the daily course of the temperature but responds to a long term trend. This behaviour dampens abrupt changes and provides a more stable biological system dynamics with less fluctuation. This means that the actual state of a plant does not entirely depend on the instantaneous value of the influencing parameter, but is determined by the cumulative effect of a previous period. The length of this influential time interval can be on the order of days, and is called hereafter the "*time of influence"* (t_{infl}).

The length of t_{infl} can also change, depending on environmental factors. To solve this problem, we calculated *S* as the linear regression of *m* against the environmental variable with many different t_{infl} to find that time interval which minimizes the variance, and therefore best describes the perceived change (see section 3.5.5).

2.3 The influence of the environment on the sensitivity

If the *sensitivity* (*S*) changes over time, we can relate its change to the course of other environmental factors. With sufficient correlation and if logic doesn't prove otherwise, we may assume that the influencing factor has been found (or at least one of them). In this paper we demonstrate that soil moisture has a good agreement with *sensitivity* changes at some selected wavelength pairs and thus these wavelengths are suitable for the indication of drought stress.

3 MATERIALS AND METHODS

3.1 Site conditions

Leaf samples were collected at the Magasbérc Artificial Drought Experiment in the Sopron Mountains (N47°39'14", E16°27'34"), Hungary, from two 64-year-old beech trees (*Fagus sylvatica*) and two sessile oak trees (*Quercus petraea*). Slight drought (soil moisture deficit) was simulated at a portion of the area by building a roof of plastic foil on wooden frames 1 m above the ground, which excluded precipitation. The treated area was already separated in 2012 below ground by plastic sheets buried in a 1 m deep trench, to cut far reaching roots and prevent possible horizontal water movement. In addition, the site is located on a hilltop where not much surface or subsurface flow is expected so that the treated trees could be isolated from any water supply.

We collected leaf samples 9 times between 11th of July and 30th of September 2014, with a sampling interval of about 2 weeks. The covering roof was assembled after the third sampling and thus, after that time, the treated area received no precipitation, which resulted in continuously decreasing soil moisture. In contrast the control area received the subsequent rainfalls and its soil moisture recovered after an intense decrease in July, thanks to the rainy and cold weather in August *(Figure 1)*. Except for soil moisture, all the other environmental factors acted equally on the trees.

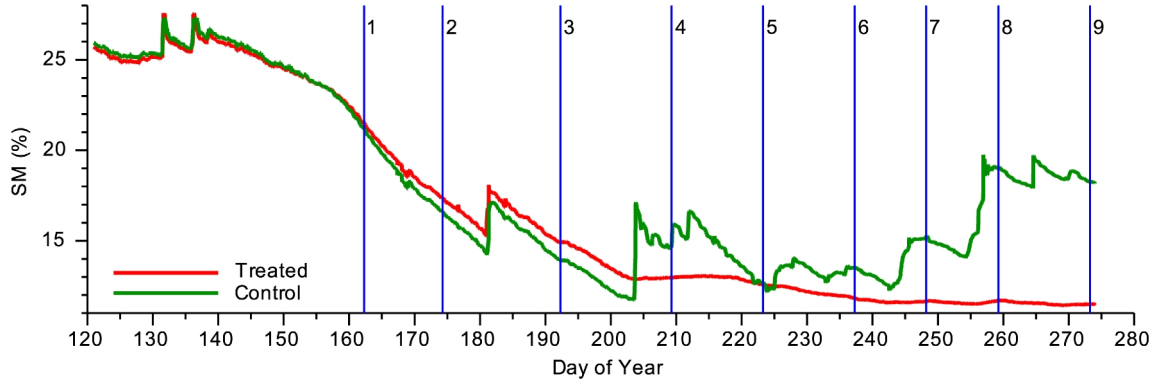

Figure 1. Time series of total soil moisture (SM) at the Treated and the Control plot. Blue vertical lines show the time of sample collection.

3.2 Sampling protocol

We collected the leaf samples in the morning from the upper part of the canopy, using rope technique. We cut a small branch containing at least 7 healthy leaves from 1 treated and 1 control tree of both species, hereafter denoted as TB (Treated Beech), CB (Control Beech), TO (Treated Oak) and CO (Control Oak). The cut branches were placed immediately into water and processing began no more than 1 hour after sample collection. Experience shows that this procedure minimizes the impact of cutting off the branches on the measurement results.

3.3 Environmental data

Meteorological parameters and soil moisture were continuously monitored with a 5 minute data logging interval at the site and a nearby (400 m) micrometeorological tower. Soil moisture was measured by EC-5 sensors (Decagon Devices Inc., USA) close to the sampled trees, buried at 5 depths (10-20-30-50-90 cm). We calculated the total soil moisture (*SM*) by a weighted mean of the 5 data. Air Temperature (*T*) and relative humidity was measured by HMP155 sensors (Vaisala, Finland) above the canopy. From this data we calculated Vapour Pressure Deficit (*VPD*) after Hardy (1998), which is the difference between the actual water vapour pressure and the saturation water vapour pressure at a particular temperature. Unlike relative humidity, Vapour Pressure Deficit has a simple nearly straight-line relationship to the rate of evapotranspiration: as *VPD* increases the plant needs to draw more water from its roots, therefore it is a good indicator of the evaporative demand.

3.4 Reflectance spectra

We measured the reflectance spectra of the leaves (7 by each tree) in the UV-VIS range of 200-1400 nm and 2 nm resolution with a Shimadzu UV-2600 spectrophotometer, and in the IR range of 700-400 0cm^{-1} and 1 cm^{-1} resolution with a Shimadzu IRAffinity-1 spectrophotometer equipped with an HATR-10 total reflection accessory (Shimadzu Corp.). The wavenumber scale (cm^{-1}) of this second instrument was converted to nm scale (2500-14940 nm) to avoid the confusion of scales on the graphs. The reflectance spectra of each leaf was smoothed by a 10 nm wide moving average, and the Standard Normal Variate (SNV) transformation was used to pre-process the data.

3.5 Data evaluation

Data processing and evaluation were done in Scilab 5.4.1 (Scilab Enterprises), and the covariance analysis and grouped linear regression were carried out in StatsDirect.

3.5.1 Selection of wavelength pairs

A sample set of 7 reflectance spectra (collected at the same time from the same tree) is shown in *Figure 2* with the marks of the wavelengths demonstrated in this paper.

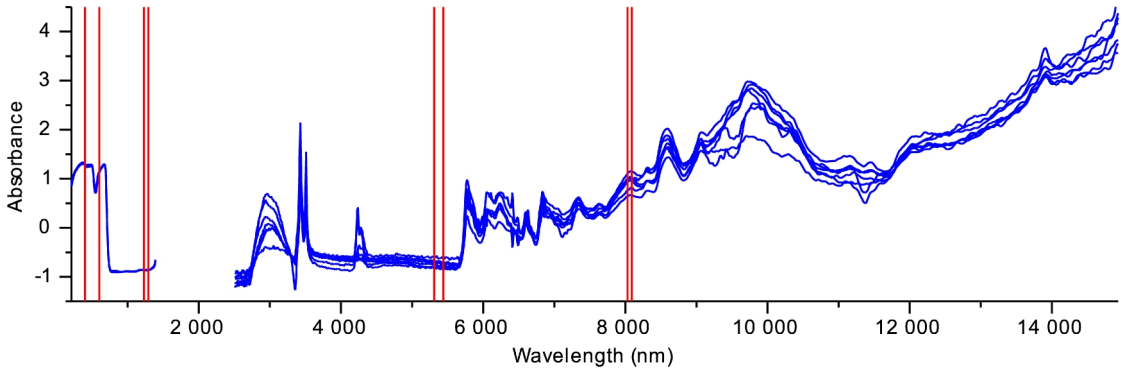

Figure 2. Sample reflectance spectra set of 7 leaves, collected from the Control Beech, at the first sampling. Red vertical lines mark the demonstrated wavelengths.

Using a 10 nm resolution, the combined UV-VIS-IR spectra provide 928,884 possible pair combinations. Of course, many neighbouring wavelengths show the effect of the same material and not all the materials show linear correlation, which we looked for. To find promising wavelength pairs, we calculated the correlation matrix of the spectra, from the 7 leaves sampled at the same time. The Pearson *R* correlation coefficient shows the strength

and sign of the linear correlation. On these autocorrelation 'maps' *(Figure 3)* those regions have been separated that show remarkable linear correlation. In each region, wavelength pairs have been selected that exhibit the highest average correlation throughout the 9 samples. However there is no guarantee at this point that these pairs carry useful information, as e.g. they may represent two characteristic wavelengths of the same material. During the evaluation process detailed below, the useless pairs were filtered out gradually. In the following sections we demonstrate the workflow using the example of the 400-600 nm wavelength pair.

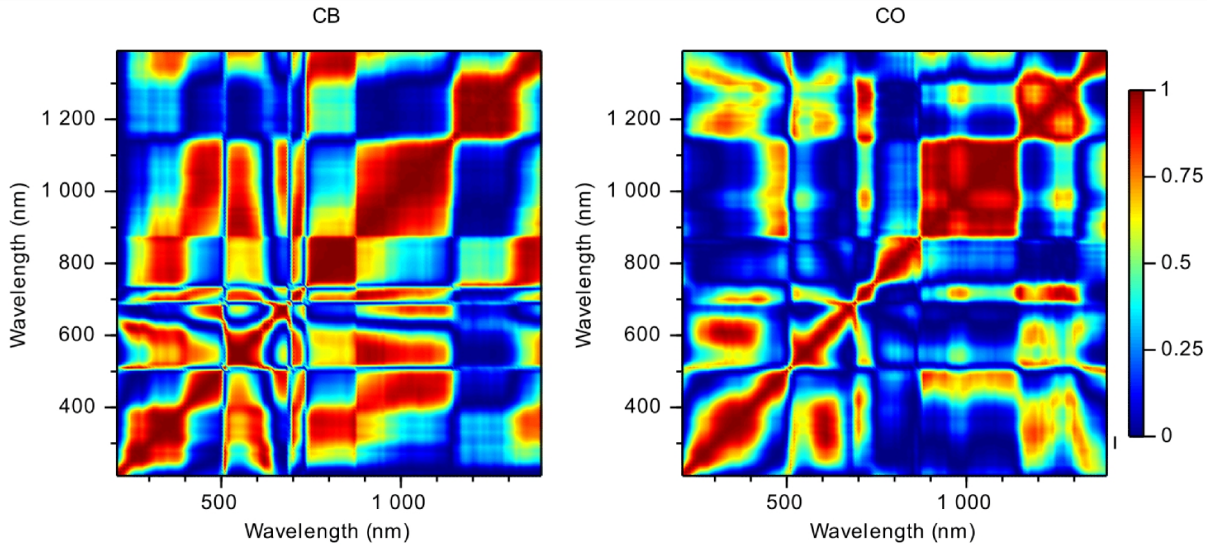

Figure 3. Two examples of autocorrelation 'maps' in the 200-1400 nm range, computed from 7 leaves of the first sampling. CB: Control Beech, CO: Control Oak. The colour shows the squared correlation coefficient (R^2): more red means stronger linear correlation.

3.5.2 State-dependent regressions

The linear regressions of the absorbance values (*Equation 3*) of the previously selected wavelength pairs were calculated for all the 9 samplings that produced a slope (m) and an intercept (b) for each sample *(Figure 4)*.

Table 2. Pair wise slope and intercept comparison of the regressions for 400-600 nm absorbance values of the Control Beech at the 9 sampling times. The upper triangle of the table contains the probability limits of significance of slope comparisons; the lower one belongs to the intercept comparison. Darker colours show more significant differences.

Slope comparison

Vertical line separation

P	sample 1	sample 2	sample 3	sample 4	sample 5	sample 6	sample 7	sample 8	sample 9
sample 1	-	0.5284	0.8538	0.0332*	0.1125	0.8961	0.8779	0.6364	0.7618
sample 2	0.3650	-	0.7548	0.1246	0.3792	0.6735	0.5839	0.4124	0.8676
sample 3	0.3156	0.8349	-	0.0841	0.2599	0.8340	0.8041	0.6272	0.9091
sample 4	0.2279	0.6401	0.7820	-	0.4450	0.1312	0.0642	0.0361*	0.1214
sample 5	0.0069**	0.0405*	0.0701	0.1574	-	0.3175	0.1954	0.1149	0.3475
sample 6	0.0269*	0.1017	0.1449	0.2697	0.8116	-	0.9770	0.9064	0.7779
sample 7	0.0005**	0.0029**	0.0063**	0.0221*	0.3104	0.2481	-	0.8377	0.7357
sample 8	0.0002**	0.0003**	0.0005**	0.0029**	0.0765	0.0595	0.4210	-	0.5762
sample 9	<0.0001**	<0.0001**	0.0005**	0.0022**	0.0473*	0.0451*	0.3138	0.8569	-

With ANCOVA (Analysis of Covariance) homogeneity test, those wavelength pairs were rejected that showed no or very little variation in the parameters *m* and *b*. The reason is that although they showed a good linear correlation, they were not sensitive to external environmental factors. *Table 2* shows an example of the significance levels of a pair wise slope and intercept comparisons. The majority of compared pairs of the regressions are below the significance criteria, therefore these regression pairs can significantly be distinguished by their slopes or their intercepts (or both).

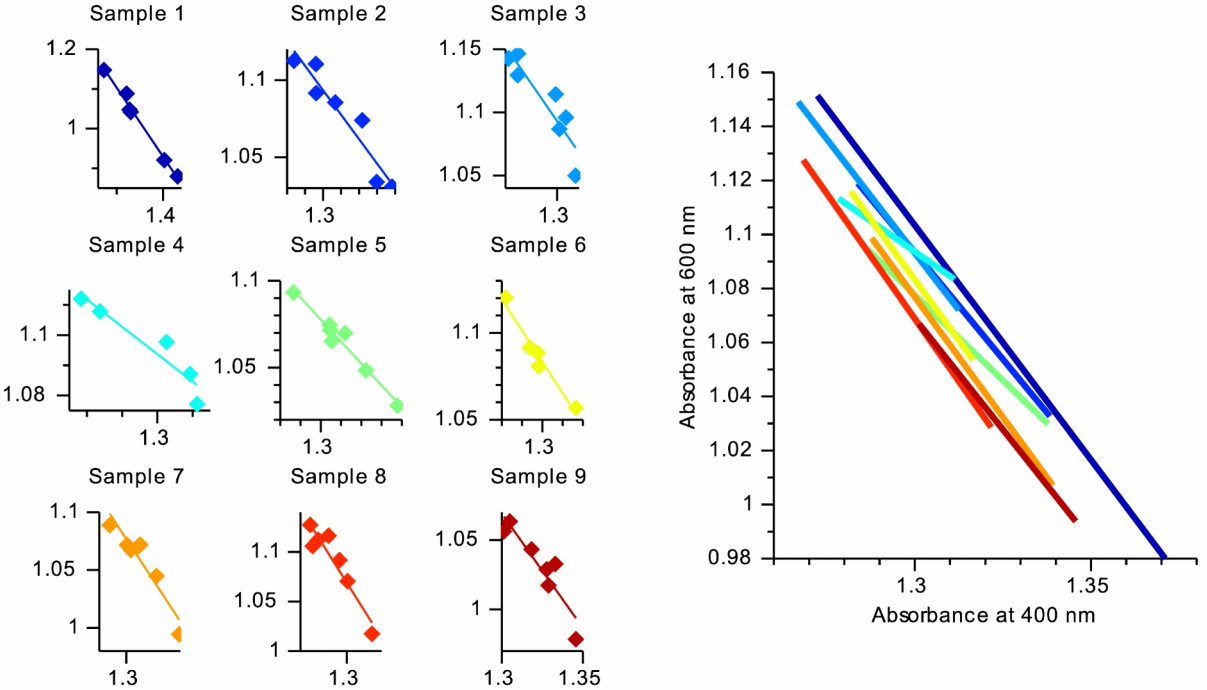

Figure 4. Example of the straight line regressions for 400-600 nm absorbance values of the Control Beech at the 9 sampling times.

3.5.3 Distribution test

The absorbance values of the selected wavelength pairs were standardized with the group means and standard deviations and plotted against each other. Ideally, the scatter plot should have a unity slope and zero intercept ($m = \pm 1,\ b = 0$) and the histograms must show similar distributions (but not necessarily a normal distribution) in order to satisfy the equivalence criteria of *Equation 1*. *Figure 5* demonstrates that initial assumptions are strengthened and thus the state-dependent correlation theory can be applied.

3.5.4 Environmental data processing

It was necessary to characterise the effect of the continuously changing environment during the influencing time intervals (t_{infl}) before each sampling. Therefore, two characteristic values were calculated: the *mean* ($T_{mean}(t_{infl})$, $VPD_{mean}(t_{infl})$), and the average rate of *change,* which is obtained by fitting a straight line to the time series, and used the slope (or derivative) of this line as an indicator of the intensity of the change ($T_{change}(t_{infl})$, $VPD_{change}(t_{infl})$). E.g. $T_{change}(3) = -1.5$ °C/day means, that during the influencing 3 days before sampling, the cooling was an average 1.5 °C per day. But the exact length of the time interval was not previously known and therefore representative values (*mean* and *change*) were calculated for a series of different intervals, e.g. $T_{change}(t)$, where t ranges between 2 to 12 days with 1 hour resolution, which includes every possible value of the parameter t_{infl}.

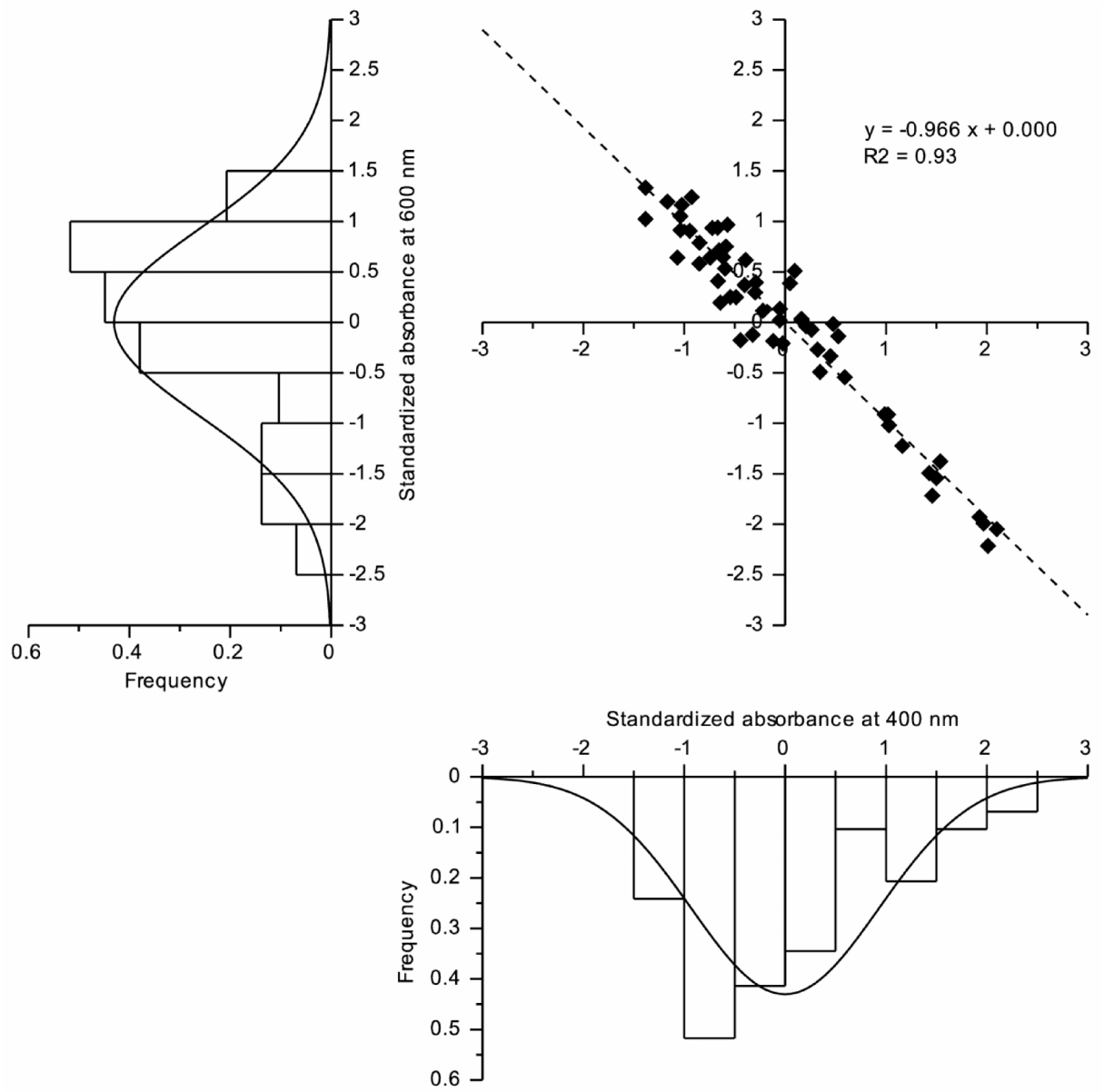

Figure 5. Control Beech 400-600 nm standardized absorbance values and their relative frequency distribution.

3.5.5 Sensitivity (S) and time of influence (t_{infl})

As defined before, the *S* is the *sensitivity* of the regression parameters (*m* and *b*) to environmental conditions. Assuming constant sensitivity, if the slope *m* of a state-dependent regression is plotted against the environmental factor e.g. T_{change}, a derived straight line may be obtained. The slope of this straight line is the *sensitivity* related to temperature *change* ($S_{Tchange}$). It shows how the state-dependent regression of the selected absorbances changes, when the weather is warming or cooling. If all the slopes of the state-dependent regressions fit to a common line, then the light absorbances at those wavelengths are not sensitive to any additional environmental stress factor, because the *sensitivity* is stable ($S_{Tchange} = const.$). On the contrary, significant changes of *S* have been sought that can be used as an indicator of environmental stress. To investigate the possible changes of *S* as time passes, the samplings were grouped into shorter *periods*, and the *S* of each *period* was computed individually. Since there were only 9 samplings, 6 overlapping *periods* (*P*) were created from groups of 4 subsequent samplings, e.g. P_1: sample 1-2-3-4, P_2: sample 2-3-4-5, P_3: sample 3-4-5-6, etc.

The *time of influence* (t_{infl}) is the time interval before the sampling that describes the observed state with the highest probability. To find this time, for each *period* the Pearson *R* correlation coefficient was calculated for all the cases of *m* versus e.g. $T_{change}(t)$, where the latter is the characteristic value of the environmental parameter calculated at every possible t_{infl} (2-12 day). Graphically, it is equivalent to fitting a straight line to the measured *m* vs. $T_{change}(t)$ at all the possible t_{infl}, and *R* describes the goodness of fit. The change of this correlation coefficient (*R*) against time (*t*) is shown in *Figure 6.A* for all 6 *periods*. The maximum (or minimum) of this curve shows the time of the best fit and thus this time is the t_{infl}. The same concept can also be applied for other environmental variables (e.g. *VPD*) and both the *mean* and *change* values.

The t_{infl} values calculated for the different *periods* sometimes show good agreement, but many times there are some *periods* out of the 6, which produce extremely low or high values (e.g. 2.6 day in *Figure 6.A*). In theory the *time of influence* is not a fixed value, but may change as *S*, since t_{infl} is also a biological response parameter. But these extremes are probably due to a special pattern of the weather alteration that misguides the algorithm. To safely calculate the real t_{infl} for each *period*, more samplings were needed. To avoid the disturbing effect of these outliers, we assumed a constant t_{infl} during all the *periods*. This is based on the mean *R* of the 6 *periods*: the time of the maximum (or minimum) of this R_{mean} indicates the presumed common t_{infl} (*Figure 6.B*). Graphically, this t_{infl} ensures the best common fit of the 6 lines. The slopes of these 6 lines are the required *sensitivities* ($S_{Tchange}$); see *Figure 6.C*.

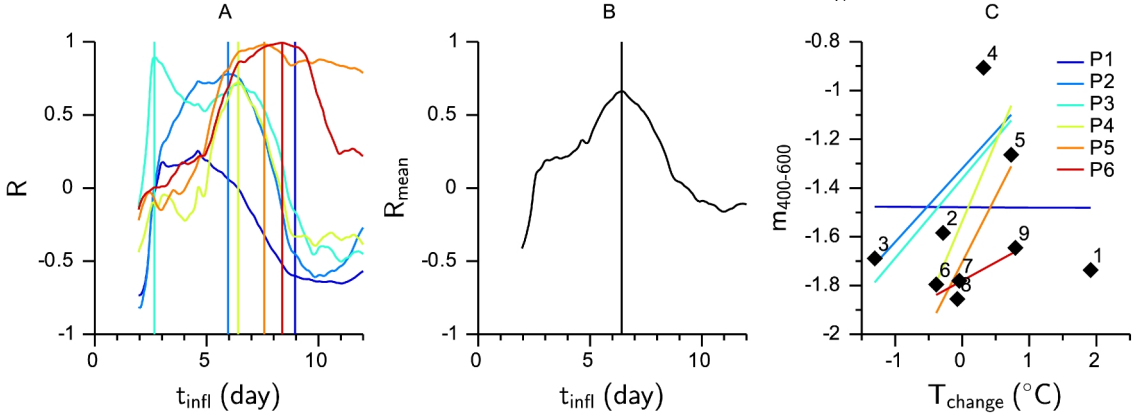

Figure 6. Control Beech 400-600 nm response to T_{change} variations.
A.) The correlation coefficients (R) vs. all possible t_{infl} for the 6 periods (P).
The maximum (or minimum) of each curve indicates the assumed t_{infl}, marked with a vertical line.
B.) The mean of the 6 correlation coefficients (R_{mean}). Its maximum indicates the common t_{infl}.
C.) m vs. $T_{change}(t_{infl})$ with the regression lines of the 6 periods. The slopes of these 6 lines are the sensitivities of the periods ($S_{Tchange}$).

3.5.6 Changing sensitivity in response to environmental stress

We needed to describe the overall effect of environmental conditions which may induce a stress syndrome in the plants. We calculated the mean values of the main environmental variables (*SM, T* and *VPD*) during the presumed common t_{infl} before every sampling, and from these ones, the *period means* were computed for the 6 *periods*. In this way, for every *period* 3 environmental factors ($SM_{period\text{-}mean}$, $T_{period\text{-}mean}$, $VPD_{period\text{-}mean}$) and a *sensitivity* (*S*) were obtained. Plotting *S* against the *period means* of the environmental factors, characteristic curves are revealed. The first graph in *Figure 6* shows that with decreasing soil moisture the *sensitivity* increases (negative slope decreases) which can also be seen in *Figure 5.C* as more steep lines. Similarly, with increasing soil moisture the *sensitivity* decreases as expected. On the contrary, the *sensitivity* shows no clear connection to the temperature or the vapour pressure deficit (*Figure 7. T and VPD*).

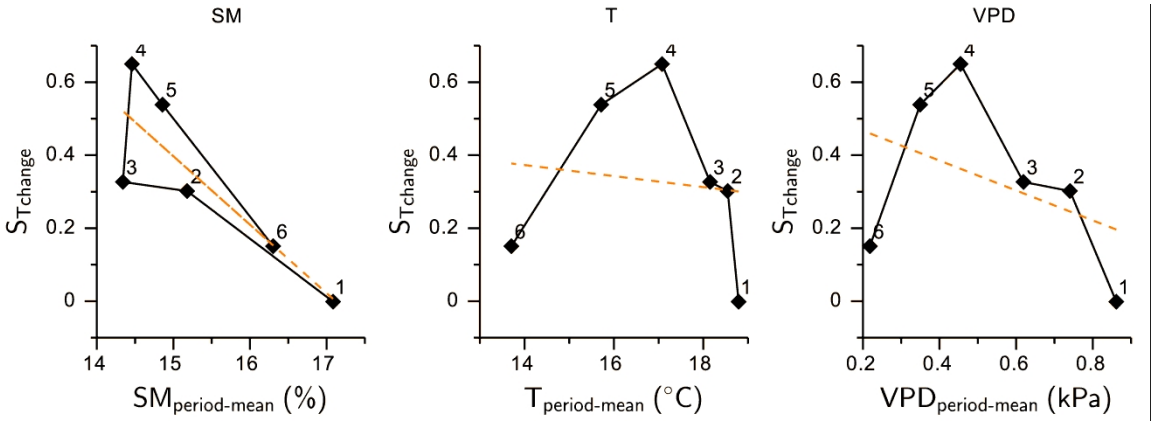

Figure 7. Control Beech 400-600 nm sensitivity for temperature change ($S_{Tchange}$) during the 6 periods (identified by numbers) vs. the environmental variables: SM - Soil moisture, T - Mean temperature, VPD - Vapour Pressure Deficit.

4 RESULTS AND DISCUSSION

Applying the previously described method, wavelength pairs that showed systematic *sensitivity* changes under drought stress were selected.

There are wavelengths which work well for both species, e.g. 400-600 nm, which is presented in *Figure 8*. Here, the regression parameter ($m_{400\text{-}600}$) varies in response to the average temperature *change* (T_{change}). The *sensitivity* of the regression in the 6 *periods* is expressed by the *sensitivity for temperature change* ($S_{Tchange}$). This $S_{Tchange}$ is plotted against the average soil moisture ($SM_{period\text{-}mean}$), which shows that in beech trees (*Figure 8 left*) the *sensitivity* increases with decreasing soil moisture (increasing drought). This means if the trees are under stress, the change of $m_{400\text{-}600}$ is bigger for the same amount of temperature change. The *sensitivities* of control beech (CB) show a nearly linear relationship with the soil moisture. The *sensitivities* of the treated beech (TB) show less change for a while, but below a certain soil moisture content (< 13%) they increase considerably.

The same seems to be true for the oaks (*Figure 8 right*); the only difference is the sign of the *sensitivity*. This negative sign means that for temperature increase (warming), oak trees raise the absolute magnitude of $m_{400\text{-}600}$. On the contrary, beech trees lessen the absolute magnitude of $m_{400\text{-}600}$ under the same circumstances. What matters is not the sign, but the magnitude of the *sensitivity*, which increases with the decreasing soil moisture as expected, signalling greater stress. If the wavelengths for the calculation of *m* are simply exchanged (e.g. not 400-600 nm, but 600-400 nm), the sign of *S* reverses.

Regressions of wavelength pairs, which can express *sensitivity* to the VPD_{change} are also be found. An example is shown with the beech trees in *Figure 9,* measured at 1230-1290 nm.

Not only the visible or near infrared range can be informative, but sensitive wavelengths in the middle infrared region can also be identified. An example for the oak trees at 5310-5440 nm (1883-1838 cm^{-1}), and for the beech trees at 8030-8090 nm (1245-1236 cm^{-1}) is depicted in *Figure 10*. Both regressions of wavelength pairs are *sensitive* to the rate of temperature *change* (T_{change}). These regressions show behaviour similar to the previously detailed examples.

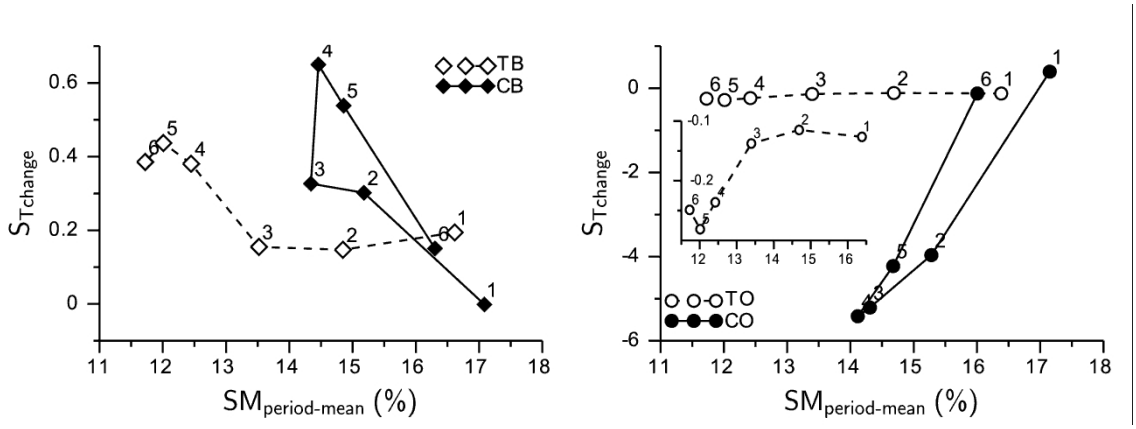

Figure 8. Beech (left) and Oak (right) 400–600 nm sensitivity ($S_{Tchange}$) vs. average Soil Moisture ($SM_{period-average}$) during the 6 periods. $S_{Tchange}$ is the sensitivity of $m_{400-600}$ to T_{change} variations. TB: Treated Beech, CB: Control Beech, TO: Treated Oak, CO: Control Oak.

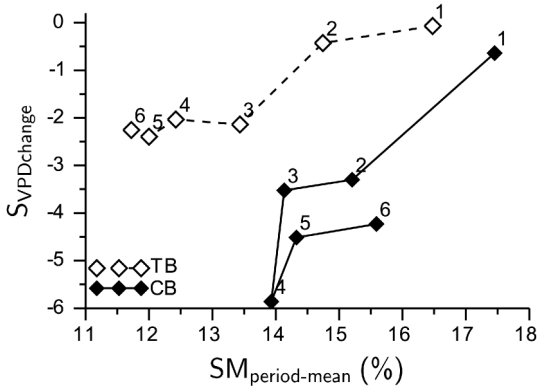

Figure 9. Beech 1230-1290 nm sensitivity ($S_{VPDchange}$) vs. average Soil Moisture ($SM_{period-average}$) during the 6 periods. $S_{VPDchange}$ is the sensitivity of $m_{1230-1290}$ to VPD change variations. CB: Control Beech, TB: Treated Beech.

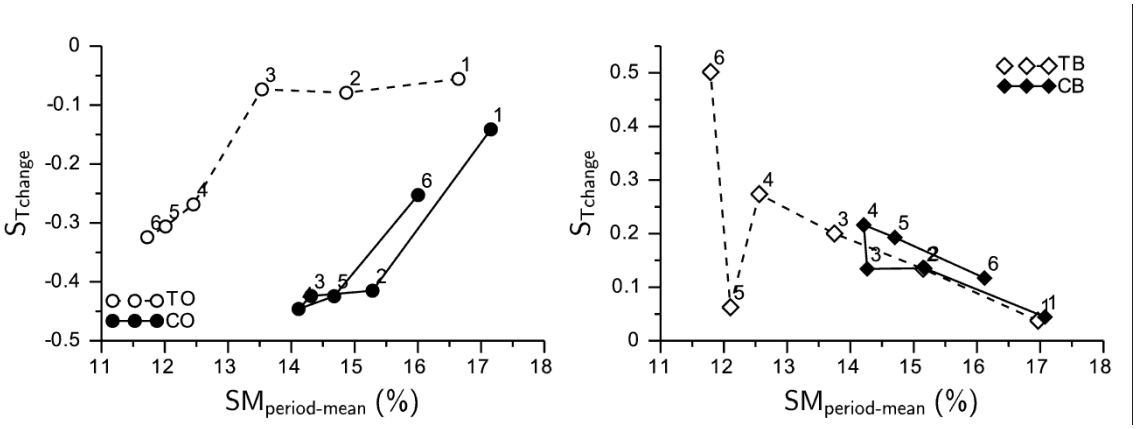

Figure 10. Oak 5310-5440 nm (left) and Beech 8030-8090 nm (right) sensitivity ($S_{Tchange}$) vs. average Soil Moisture ($SM_{period-average}$) during the 6 periods. $S_{Tchange}$ is the sensitivity of $m_{5310-5440}$ and $m_{8030-8090}$ to T_{change} variations, respectively. TO: Treated Oak, CO: Control Oak, TB: Treated Beech, CB: Control Beech.

At 400 nm and 600 nm wavelengths the absorbance intensities are mainly affected by the photosynthetic pigments (chlorophylls, xanthophylls, carotenoids, etc.). At 400 nm almost all of the pigments contribute to the resultant absorption, but at 600 nm the absorbance is determined mainly by chlorophylls. Thus the $m_{400\text{-}600}$ slope changes of the state-dependent regressions indicate the variation in the ratio of chlorophylls compared to the total pigment content, and this variation is sensitive to the environmental parameters such as temperature and soil moisture. Between 1200 and 1300 nm, water and the lingo-cellulose system are the significant influencing factors for the light absorption. At even higher wavelengths, the overtones of vibration resonances of the molecules prevail the absorbance spectra.

However, to successfully use the state-dependent regression method, the exact knowledge of the underlying materials is not required and in many cases it is not even possible due to the high number of different bio-materials that shape the spectra at a given wavelength.

The wavelengths presented in this paper are not meant to be a process description, but to serve as the proof of concept. To fine tune the method for practical application more investigation is needed.

5 SUMMARY

Middle-aged beech and sessile oak trees have been investigated while slight drought (soil moisture deficit) has been simulated at half of the trees. Environmental parameters have been continuously monitored and the foliages have been sampled regularly to obtain UV-VIS-IR reflectance spectra of the leaves.

The state-dependent correlations at particular wavelength pairs in the reflectance spectra of foliage are sensitive to environmental variations. Changes in the environmental parameters, such as those of temperature or vapour pressure deficit, cause significant variations in the slope of the regression straight lines. The *sensitivity* of this variation, e.g. how big the slope change is for a given temperature rising, can be expressed by the *sensitivity for temperature change*. This *sensitivity*, in turn, varies with the soil moisture; the bigger the water deficit, the greater the absolute magnitude of the *sensitivity*. Therefore the slopes of the state-dependent regressions of some selected wavelengths are good indicators of the available soil moisture.

If the selected wavelengths are not directly sensitive to the water content of leaves, but measure some synthesized bio-materials, then the slopes represent the underlying metabolic regulation. In this way, the changes of *sensitivity* reflect the changes of metabolic regulation and its stability. The state and the stability of the regulation define the level of drought stress, summing up the long term effects of the environment.

This method applies the approach of state-dependent correlation for data analysis. This kind of correlation, due to the synchronous regulation of certain bio-material pairs, can be found in many biochemical processes. The exact qualification of materials influencing the reflectance spectra may be desirable but is not necessarily required. This is because it is not the material qualities but their amounts that determine the regression relationship at the selected wavelengths. The existence of state dependent correlation can be proved statistically without a priori knowing the materials involved. Moreover, as previous studies suggest, it might be utilized to assess not only drought stress, but many other environmental stress factors, too. However, it requires further investigation.

Acknowledgements: The investigation was funded by the 4.2.2.B-10/1-2010-0018 “Talentum” project, the 4.2.2.A-11/1/KONV-2012-0013 ”Agrárklíma” project and the VKSZ_12-1-2013-0034 “Agrárklíma 2” project. Sample collection, multivariate analysis,

programming and evaluation were done by Attila Eredics and the concept of model and investigation were offered by Zsolt István Németh. We wish to thank Rita Rákosa for the spectrophotometric measurements, Ervin Rasztovits and Norbert Móricz for the construction of the MAD Experiment and the help in sample collection, and Péter Vig for the meteorological data.

REFERENCES

ADAMS III, W. W. – DEMMIG-ADAMS, B. (1992): Operation of the xanthophyll cycle in higher plants in response to diurnal changes in incident sunlight. Planta 186(3): 390–398.

ALDAKHEEL, Y. Y. (2011): Assessing NDVI spatial pattern as related to irrigation and soil salinity management in Al-Hassa Oasis, Saudi Arabia. Journal of the Indian Society of Remote Sensing 39(2): 171–180.

BADÁCZY, D. Z. – NÉMETH, K. E. – KOCSIS, R. – NÉMETH, ZS. I. (2011): Interaction between plant and environment revealed by the concept of state-dependent correlation, 4th European Conference on Chemistry for Life Sciences (31 Aug – 3 Sept, 2011, Budapest, Hungary), Medimond International Proceedings, Bologna, Italy. 7–10.

BARET, F. – ANDRIEU, B. – GUYOT, G. (1988): A simple model for leaf optical properties in visible and near-infrared: application to the analysis of spectral shifts determinism. In: Applications of Chlorophyll Fluorescene in Photosynthesis Research, Stress Physiology, Hydrobiology and Remote Sensing. Springer, Netherlands. 345–351.

BARNES, J. D. – BALAGUER, L. – MANRIQUE, E. – ELVIRA, S. – DAVISON, A. W. (1992): A reappraisal of the use of DMSO for the extraction and determination of chlorophylls a and b in lichens and higher plants. Environmental and Experimental Botany 32(2): 85–100.

BROGE, N. H. – LEBLANC, E. (2001): Comparing prediction power and stability of broadband and hyperspectral vegetation indices for estimation of green leaf area index and canopy chlorophyll density. Remote sensing of environment 76(2): 156–172.

BUSHEVA, M. – GARAB, G. – LIKER, E. – TÓTH, Z. – SZÈLL, M. – NAGY, F. (1991): Diurnal Fluctuations in the Content and Functional Properties of the Light Harvesting Chlorophyll a/b Complex in Thylakoid Membranes Correlation with the Diurnal Rhythm of the mRNA Level. Plant physiology 95(4): 997–1003.

CARTER, G. A. (1994): Ratios of leaf reflectances in narrow wavebands as indicators of plant stress. Remote sensing 15(3): 697–703.

CRAIN, J. – ORTIZ-MONASTERIO, I. – RAUN, B. (2012): Evaluation of a Reduced Cost Active NDVI Sensor for Crop Nutrient Management. Journal of Sensors 2012: 1-10.

DAUGHTRY, C. S. T. – WALTHALL, C. L. – KIM, M. S. – DE COLSTOUN, E. B. – MCMURTREY, J. E. (2000): Estimating corn leaf chlorophyll concentration from leaf and canopy reflectance. Remote sensing of Environment 74(2): 229–239.

DIXON, M. A. – TYREE, M. T. (1984): A new stem hygrometer, corrected for temperature gradients and calibrated against the pressure bomb. Plant, Cell & Environment 7(9): 693–697.

EITEL, J. U. H. – LONG, D. S. – GESSLER, P. E. – SMITH, A. M. S. (2007): Using in-situ measurements to evaluate the new RapidEye™ satellite series for prediction of wheat nitrogen status. International Journal of Remote Sensing 28(18): 4183–4190.

FILELLA, I. – PEÑUELAS, J. (1994): The red edge position and shape as indicators of plant chlorophyll content, biomass and hydric status. International Journal of Remote Sensing 15(7): 1459-1470.

GALVÃO, L. S. – FORMAGGIO, A. R. – TISOT, D. A. (2005): Discrimination of sugarcane varieties in Southeastern Brazil with EO-1 Hyperion data. Remote Sensing of Environment 94(4): 523–534.

GAMON, J. A. – FIELD, C. B. – GOULDEN, M. L. – GRIFFIN, K. L. – HARTLEY, A. E. – JOEL, G. – PEÑUELAS, J. – VALENTINI, R. (1995): Relationships between NDVI, canopy structure, and photosynthesis in three Californian vegetation types. Ecological Applications 1995: 28–41.

GAMON, J. A. – PENUELAS, J. – FIELD, C. B. (1992): A narrow-waveband spectral index that tracks diurnal changes in photosynthetic efficiency. Remote Sensing of environment, 41(1): 35–44.

GAO, B. C. (1996): NDWI – a normalized difference water index for remote sensing of vegetation liquid water from space. Remote sensing of environment 58(3): 257–266.

GITELSON, A. A. – MERZLYAK, M. N. (1997): Remote estimation of chlorophyll content in higher plant leaves. International Journal of Remote Sensing 18(12): 2691–2697.

HABOUDANE, D. – MILLER, J. R. – PATTEY, E. – ZARCO-TEJADA, P. J. – STRACHAN, I. B. (2004): Hyperspectral vegetation indices and novel algorithms for predicting green LAI of crop canopies: Modeling and validation in the context of precision agriculture. Remote sensing of environment 90(3): 337–352.

HABOUDANE, D. – MILLER, J. R. – TREMBLAY, N. – ZARCO-TEJADA, P. J. – DEXTRAZE, L. (2002): Integrated narrow-band vegetation indices for prediction of crop chlorophyll content for application to precision agriculture. Remote sensing of environment 81(2): 416–426.

HARDY, B. (1998): ITS-90 Formulations for Vapor Pressure, Frostpoint Temperature, Dewpoint Temperature, and Enhancement Factors in the Range -100 to +100 C. The Proceedings of the Third International Symposium on Humidity & Moisture, Teddington, London, England, April 1998: 1-8.

HENRICH, V. – KRAUSS, G. – GÖTZE, C. – SANDOW, C. (2012): IDB - www.indexdatabase.de, Entwicklung einer Datenbank für Fernerkundungsindizes. AK Fernerkundung, Bochum, 4.-5. 10. 2012. (PDF)

HUETE, A. R. (1988): A soil-adjusted vegetation index (SAVI). Remote sensing of environment 25(3): 295–309.

HUNSAKER, D. J. – FITZGERALD, G. J. – FRENCH, A. N. – CLARKE, T. R. – OTTMAN, M. J. – PINTER JR, P. J. (2007): Wheat irrigation management using multispectral crop coefficients. I. Crop evapotranspiration prediction. Trans. ASABE 50(6): 2017–2033.

JORDAN, C. F. (1969), Derivation of leaf area index from quality of light on the forest floor. Ecology 50: 663-666.

LI, J. – PU, L. – HAN– M. – ZHU, M. – ZHANG, R. – XIANG, Y. (2014): Soil salinization research in China: Advances and prospects. Journal of Geographical Sciences 24(5): 943–960.

LICHTENTHALER, H. K. (1996): Vegetation stress: an introduction to the stress concept in plants. Journal of plant physiology 148(1): 4–14.

MORIONDO, M. – MASELLI, F. – BINDI, M. (2007): A simple model of regional wheat yield based on NDVI data. European Journal of Agronomy 26(3): 266–274.

NÉMETH, ZS. I. – SÁRDI, É. – STEFANOVITS-BÁNYAI É. (2009a): State dependent correlations of biochemical variables in plants, Journal of Chemometrics 23: 197–210.

NÉMETH, ZS. I. (2009b): Növényi stressz vizsgálata és értelmezése szabályozáselméleti analógiák alapján. [Investigation and interpretation of plant stress on the basis of control theory analogies.] MTA Bolyai János Ösztöndíjkutatás (2006–2009), Zárójelentés, 35 p. (in Hungarian)

NÉMETH, ZS. I. (2013): Növényi anyagcsere alkalmazkodása a környezet tényezőinek módosulásaihoz, [The adaptation of plant metabolism to the changing environment] In: Albert L. – Bidló A. – Jancsó T. – Gribovszki Z –, Kámán O. (eds): Városok öko-környezetének komplex vizsgálata a nyugat dunántúli régióban. Nyugat-magyarországi Egyetem Kiadó, Sopron. 237-260. (in Hungarian)

PEÑUELAS, J. – FILELLA, I. (1998): Visible and near-infrared reflectance techniques for diagnosing plant physiological status. Trends in plant science 3(4): 151–156.

PEÑUELAS, J. – BARET, F. – FILELLA, I. (1995): Semi-empirical indices to assess carotenoids/chlorophyll a ratio from leaf spectral reflectance. Photosynthetica 31: 221–230.

PEÑUELAS, J. – GAMON, J. A. – FREDEEN, A. L. – MERINO, J. – FIELD, C. B. (1994): Reflectance indices associated with physiological changes in nitrogen-and water-limited sunflower leaves. Remote Sensing of Environment, 48(2): 135-146.

PEÑUELAS, J. – LLUSIA, J. – PINOL, J. – FILELLA, I. (1997a): Photochemical reflectance index and leaf photosynthetic radiation-use-efficiency assessment in Mediterranean trees. International Journal of Remote Sensing 18(13): 2863–2868.

PEÑUELAS, J. – PINOL, J. – OGAYA, R. – FILELLA, I. (1997b): Estimation of plant water concentration by the reflectance water index WI (R900/R970). International Journal of Remote Sensing 18(13): 2869–2875.

PU, R. (2008): An exploratory analysis of in situ hyperspectral data for broadleaf species recognition. The International Archives of the Photogrammetry, Remote Sensing and Spatial Information Sciences, Beijing. 255-260.

PU, R. – GE, S. – KELLY– N. M. – GONG, P. (2003): Spectral absorption features as indicators of water status in coast live oak (*Quercus agrifolia*) leaves. International Journal of Remote Sensing 24(9): 1799–1810.

QI, J. – CHEHBOUNI, A. – HUETE, A. R. – KERR, Y. H. – SOROOSHIAN, S. (1994): A modified soil adjusted vegetation index. Remote sensing of environment 48(2): 119–126.

RONDEAUX, G. – STEVEN, M. – BARET, F. (1996): Optimization of soil-adjusted vegetation indices. Remote sensing of environment 55(2): 95–107.

ROUJEAN, J. L. – BREON, F. M. (1995): Estimating PAR absorbed by vegetation from bidirectional reflectance measurements. Remote Sensing of Environment 51(3): 375–384.

ROUSE, J.W.JR. – HAAS, R.H. – SCHELL, J.A. – DEERING, D.W. (1973): Monitoring the vernal advancement and retrogradation (green wave effect) of natural vegetation. Prog. Rep. RSC 1978-1, Remote Sensing Center, Texas A&M Univ., College Station, 93 p.

SCHOLANDER, P. F. – BRADSTREET, E. D. – HEMMINGSEN, E. A. – HAMMEL, H. T. (1965): Sap Pressure in Vascular Plants: Negative hydrostatic pressure can be measured in plants. Science 148(3668): 339–346.

SHIMADA, B. M. (1958): Diurnal fluctuation in photosynthetic rate and chlorophyll "a" content of phytoplankton from eastern Pacific waters. Limnology and Oceanography 3(3): 336–339.

STONE, M. L. – SOLIE, J. B. – RAUN, W. R. – WHITNEY, R. W. – TAYLOR, S. L. – RINGER, J. D. (1996): Use of spectral radiance for correcting in-season fertilizer nitrogen deficiencies in winter wheat. Transactions of the ASAE 39(5): 1623–1631.

TAN, C. – SAMANTA, A. – JIN, X. – TONG, L. – MA, C. – GUO, W. – KNYAZIKHIN, Y. – MYNENI, R. B. (2013): Using hyperspectral vegetation indices to estimate the fraction of photosynthetically active radiation absorbed by corn canopies. International Journal of Remote Sensing 34(24): 8789–8802.

TEAL, R. K. – TUBANA, B. – GIRMA, K. – FREEMAN, K. W. – ARNALL, D. B. – WALSH, O. – RAUN, W. R. (2006): In-season prediction of corn grain yield potential using normalized difference vegetation index. Agronomy Journal 98(6): 1488–1494.

VOGELMANN, J. E. – ROCK, B. N. – MOSS, D. M. (1993): Red edge spectral measurements from sugar maple leaves. International Journal of Remote Sensing 14: 1563–1575.

ZARCO-TEJADA, P. J. – BERJÓN, A. – MILLER, J. R. (2004): Stress detection in crops with hyperspectral remote sensing and physical simulation models. Proceedings of the Airborne Imaging Spectroscopy Workshop - Bruges, 8 October 2004. 5p.

ZARCO-TEJADA, P. J. – MILLER, J. R. – NOLAND, T. L. – MOHAMMED, G. H. – SAMPSON, P. H. (2001): Scaling-up and model inversion methods with narrowband optical indices for chlorophyll content estimation in closed forest canopies with hyperspectral data. Geoscience and Remote Sensing, IEEE Transactions on Geoscience and Remote Sensing, 39(7): 1491–1507.

ZIMMERMANN, D. – REUSS, R. – WESTHOFF, M. – GEßNER, P. – BAUER, W. – BAMBERG, E. – BENTRUP, F-W. – ZIMMERMANN, U. (2008): A novel, non-invasive, online-monitoring, versatile and easy plant-based probe for measuring leaf water status. Journal of Experimental Botany 59(11): 3157–3167.